Electronic Supplementary Material (ESI) for Journal of Nanoscale.
This journal is © The Royal Society of Chemistry 2020

Electronic Supplementary Information

One-pot synthesis of Mn-Fe bimetallic oxide heterostructure as bifunctional electrodes for efficient overall water splitting

Juan Luo, Wan Hui Guo, Qing Zhang, Xiao Hu Wang, Li Shen, Hong Chuan Fu, Li Li Wu, Xiao Hui Chen, Hong Qun Luo*, and Nian Bing Li*

School of Chemistry and Chemical Engineering, Southwest University, Chongqing 400715, People's Republic of China

E-mail address: linb@swu.edu.cn (N. B. Li); luohq@swu.edu.cn (H. Q. Luo)

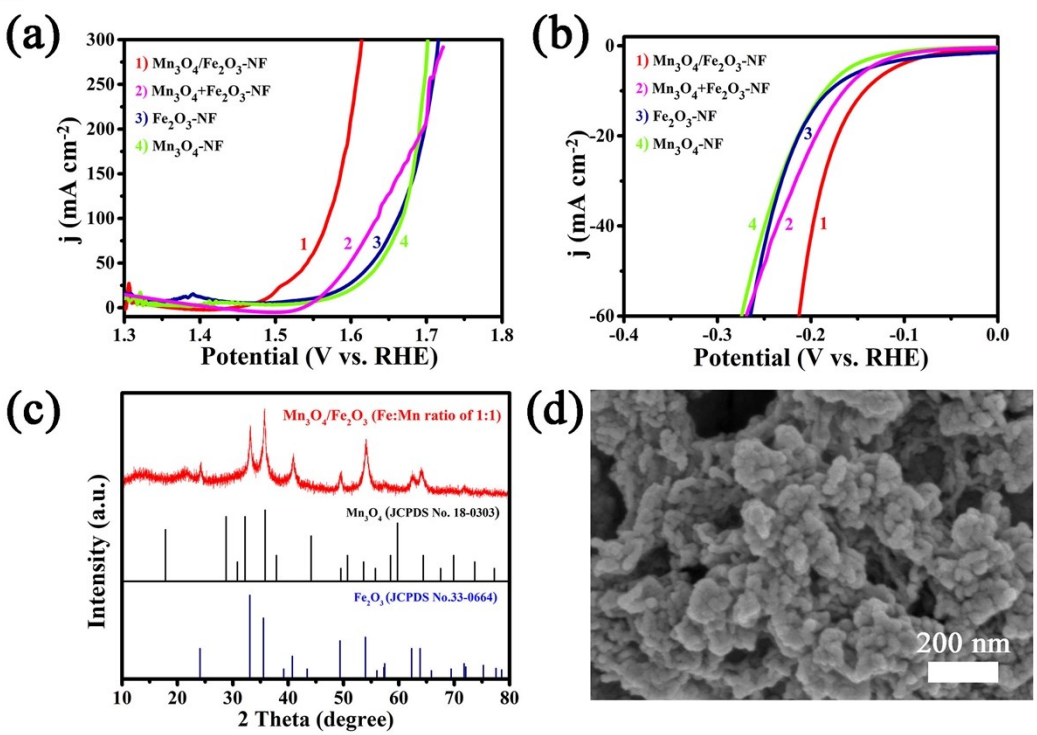

Fig. S1. (a) OER polarization curves and (b) HER polarization curves of Mn_3O_4/Fe_2O_3-NF complex, Mn_3O_4+Fe_2O_3-NF complex, Fe_2O_3-NF, and Mn_3O_4-NF in 1.0 M KOH. (c) XRD pattern and (d) SEM image of Mn_3O_4/Fe_2O_3 (Fe:Mn ratio of 1:1).

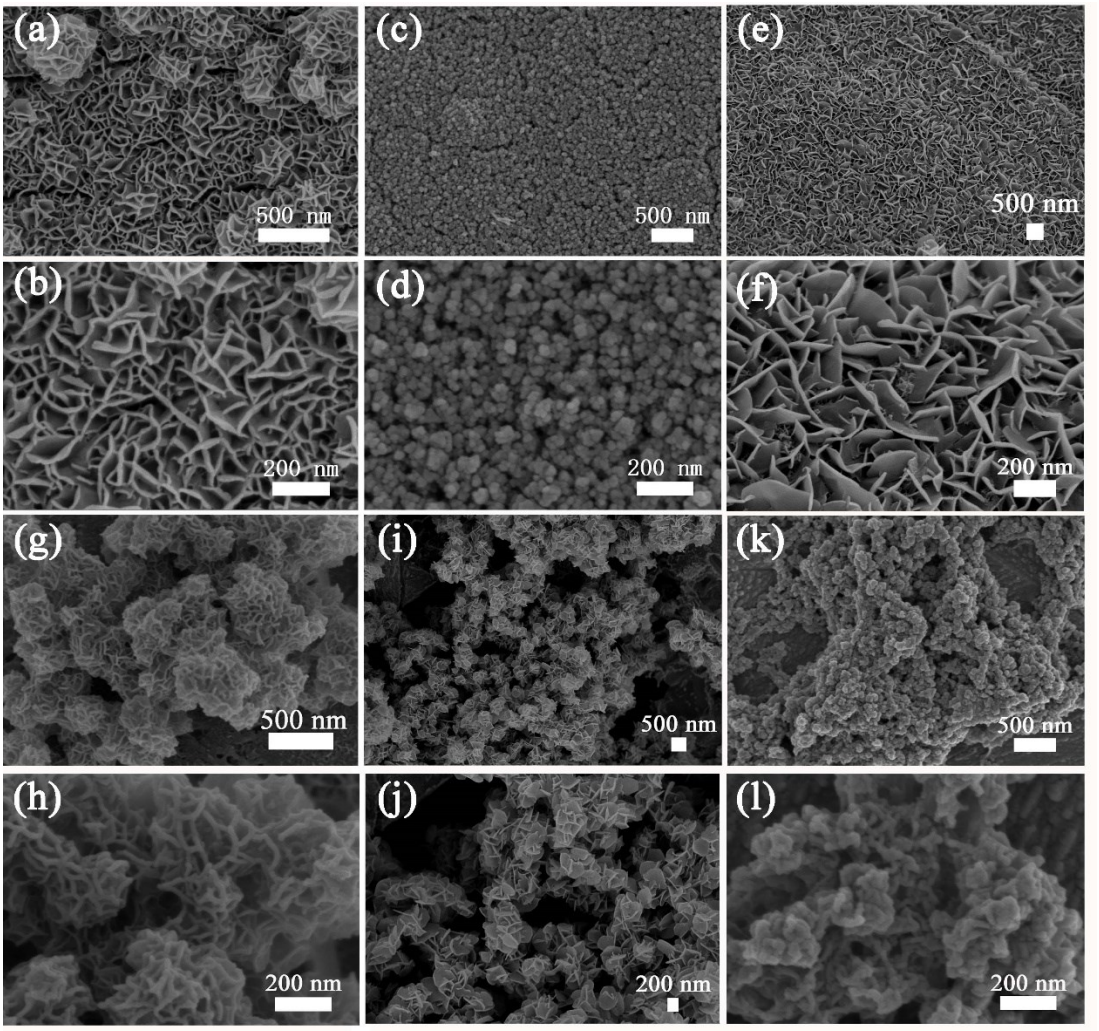

Fig. S2. SEM and magnified SEM images of MnO_2-NF (a, b), MnFeO-NF-0.2 (c, d), MnFeO-NF-0.4 (e, f), MnFeO-NF-0.6 (g, h), MnFeO-NF-0.8 (i, j), and MnFeO-NF-1 (k, l), respectively.

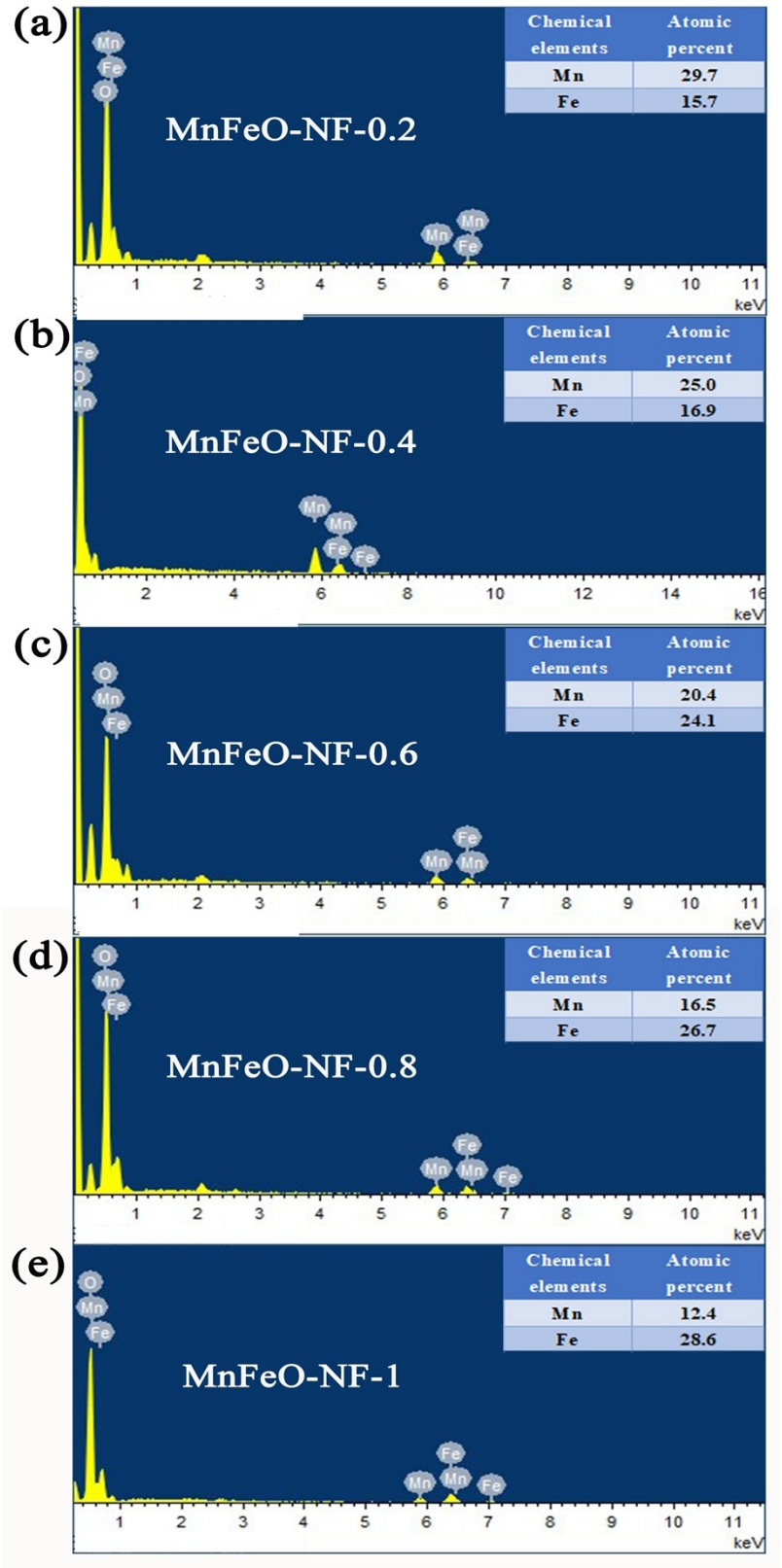

Fig. S3. EDS data of (a) MnFeO-NF-0.2, (b) MnFeO-NF-0.4, (c) MnFeO-NF-0.6, (d) MnFeO-NF-0.8, and (e) MnFeO-NF-1. Inset image is a table of atomic percent of Mn and Fe.

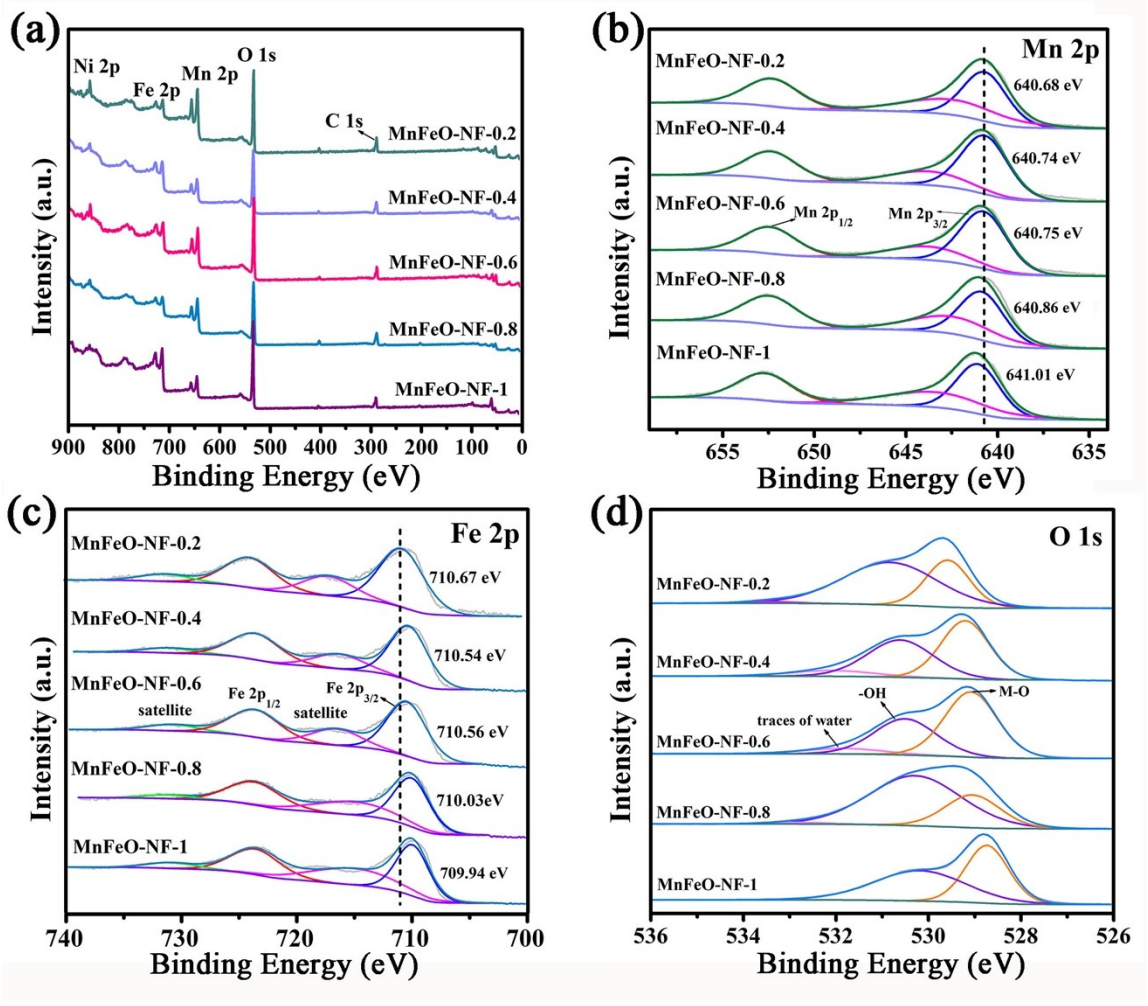

Fig. S4. (a) XPS survey of MnFeO-NF-0.2, MnFeO-NF-0.4, MnFeO-NF-0.6, MnFeO-NF-0.8, and MnFeO-NF-1. (b–d) High resolution XPS spectra of Mn 2p, Fe 2p, and O 1s.

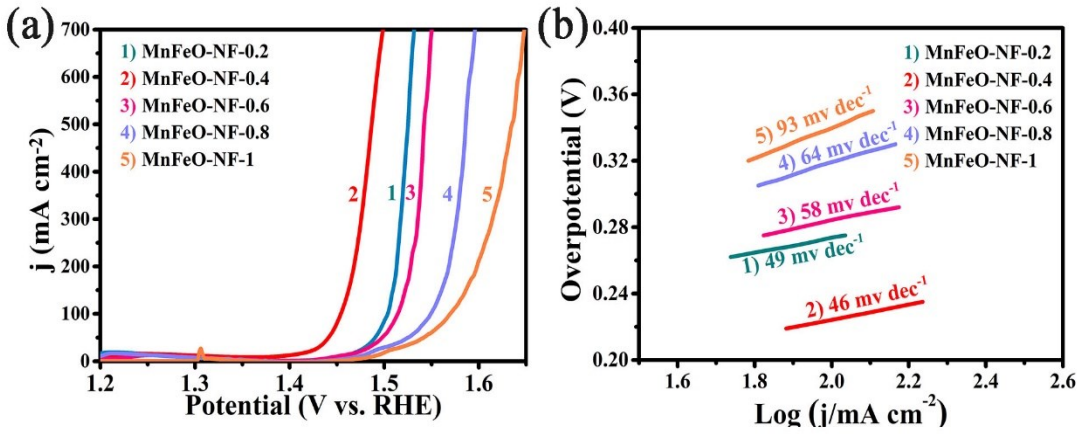

Fig. S5. (a) Polarization curves and (b) Tafel plots of MnFeO-NF-0.2, MnFeO-NF-0.4, MnFeO-NF-0.6, MnFeO-NF-0.8, and MnFeO-NF-1 in 1.0 M KOH.

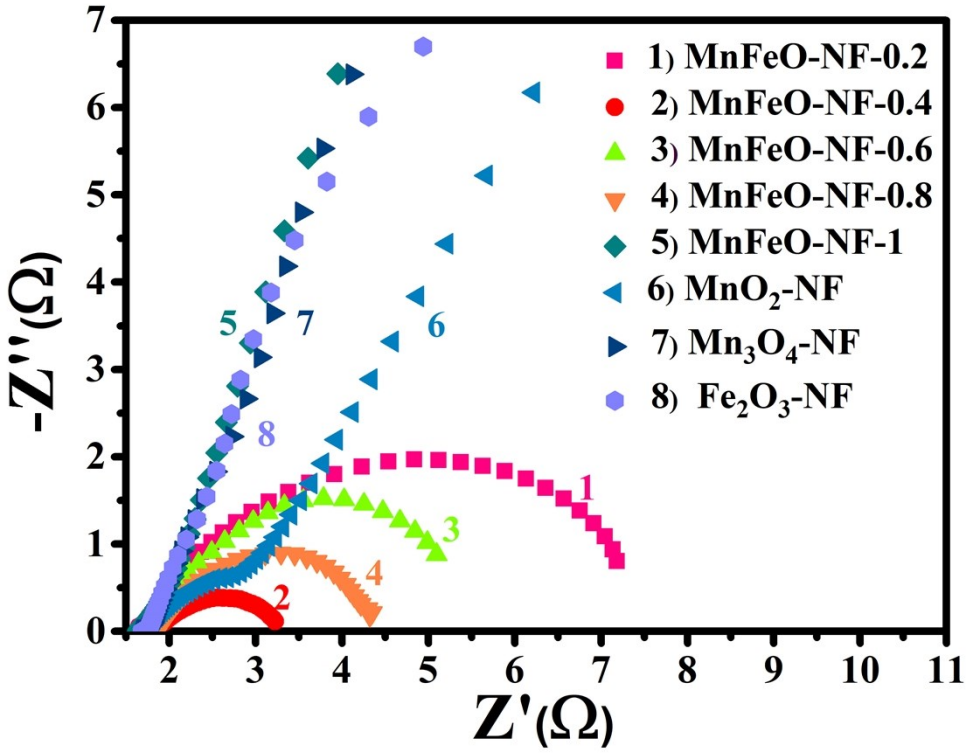

Fig. S6. EIS of MnFeO-NF-0.2, MnFeO-NF-0.4, MnFeO-NF-0.6, MnFeO-NF-0.8, MnFeO-NF-1, MnO_2-NF, Mn_3O_4-NF, and Fe_2O_3-NF at 1.533 V *vs.* RHE.

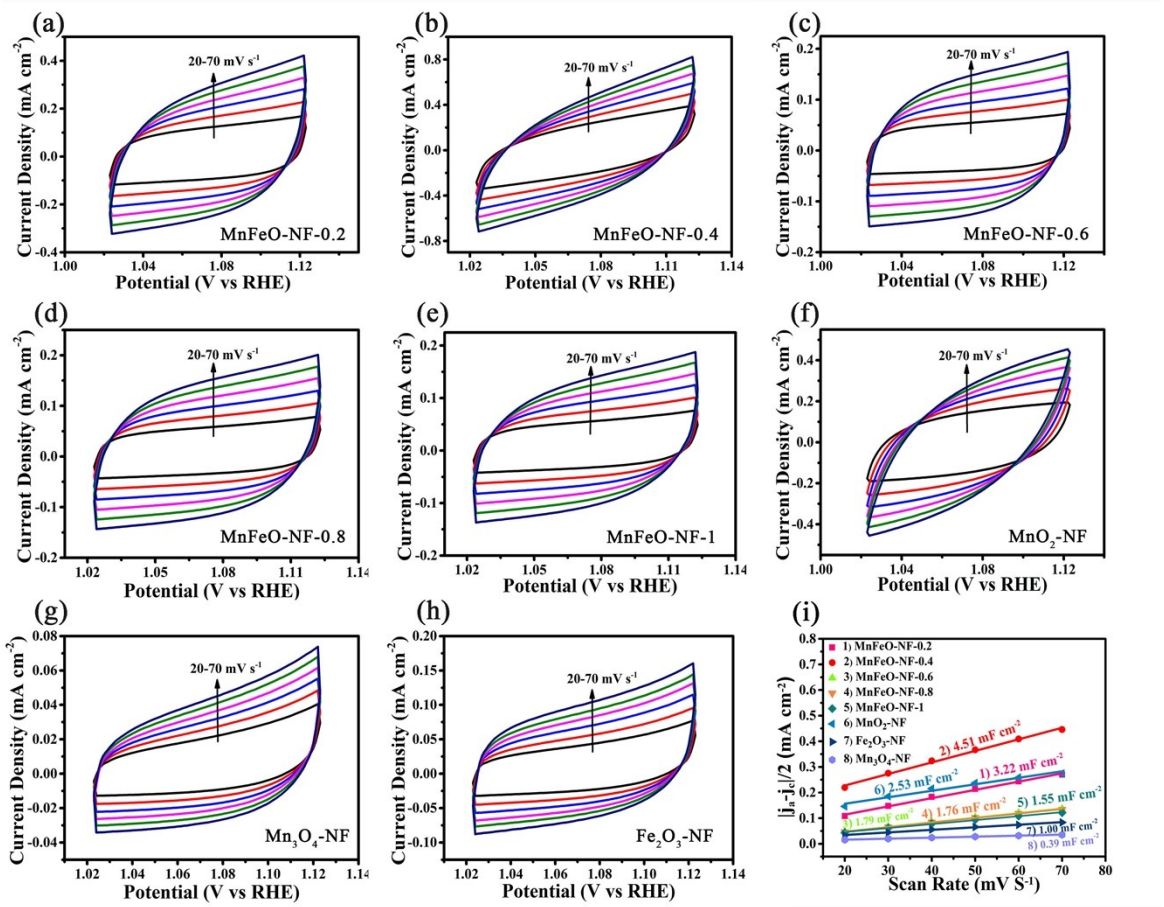

Fig. S7. CV curves at different scan rates for catalysts: (a) MnFeO-NF-0.2, (b) MnFeO-NF-0.4, (c) MnFeO-NF-0.6, (d) MnFeO-NF-0.8, (e) MnFeO-NF-1, (f) MnO_2-NF, (g) Mn_3O_4-NF, and (h) Fe_2O_3-NF, (i) Plots of capacitive currents with different scan rates for various catalysts to determine C_{dl}.

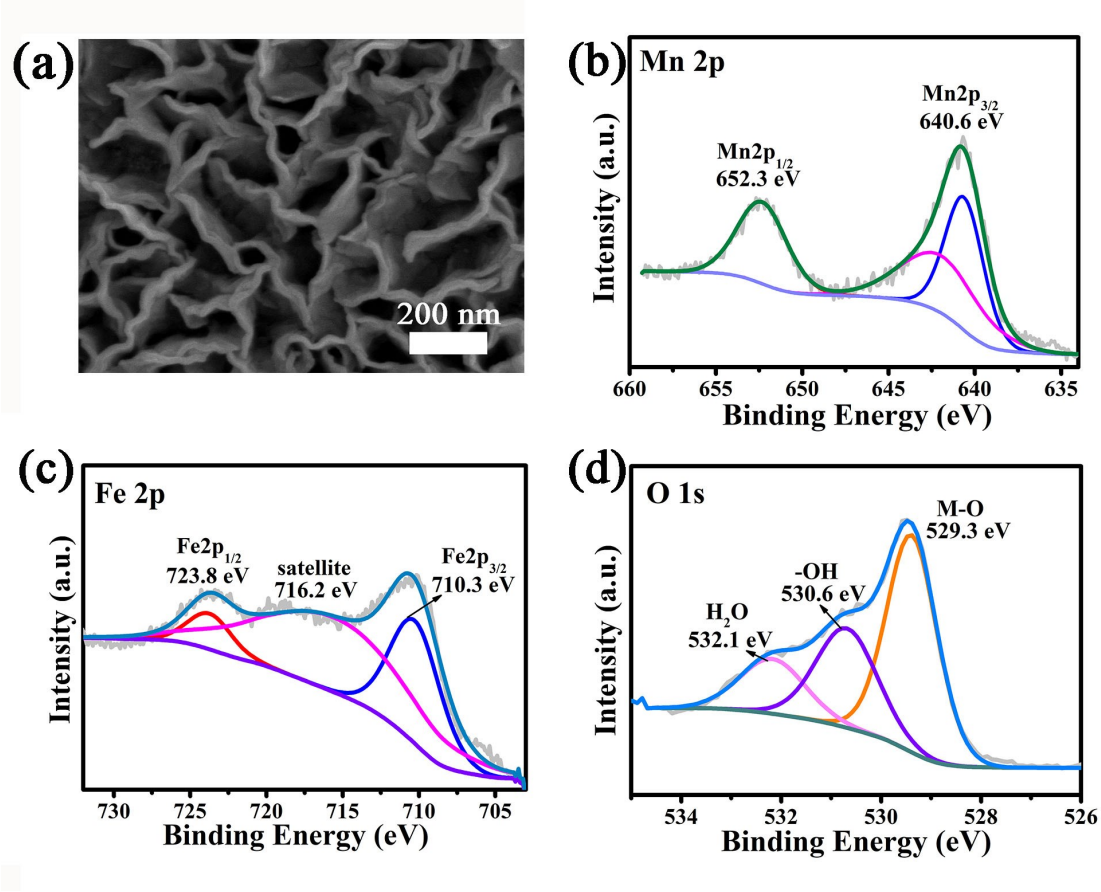

Fig. S8. (a) SEM image of MnFeO-NF-0.4 after stability test. (b–d) High resolution XPS spectra of Mn 2p, Fe 2p, and O 1s after stability test.

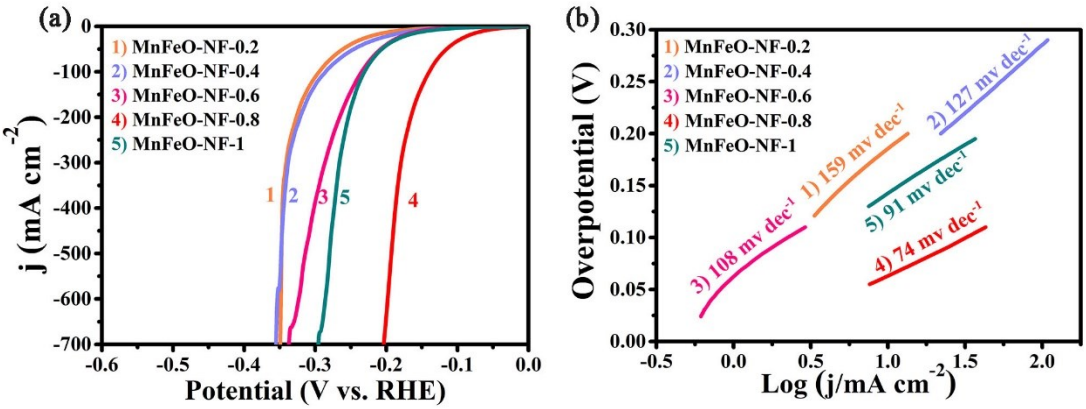

Fig. S9. (a) Polarization curves and (b) Tafel plots of MnFeO-NF-0.2, MnFeO-NF-0.4, MnFeO-NF-0.6, MnFeO-NF-0.8, and MnFeO-NF-1 in 1.0 M KOH.

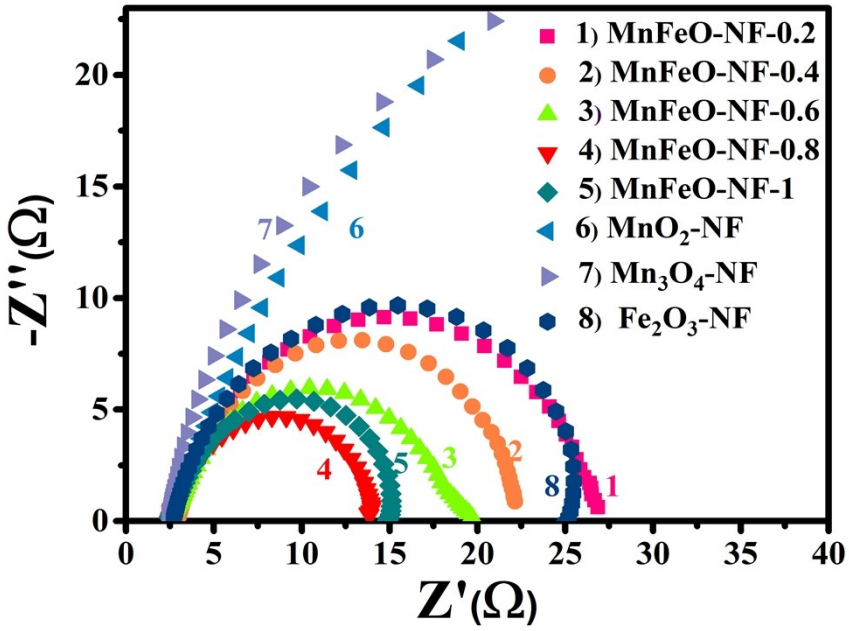

Fig. S10. EIS of MnFeO-NF-0.2, MnFeO-NF-0.4, MnFeO-NF-0.6, MnFeO-NF-0.8, MnFeO-NF-1, MnO_2-NF, Mn_3O_4-NF, and Fe_2O_3-NF at -0.177 V *vs.* RHE.

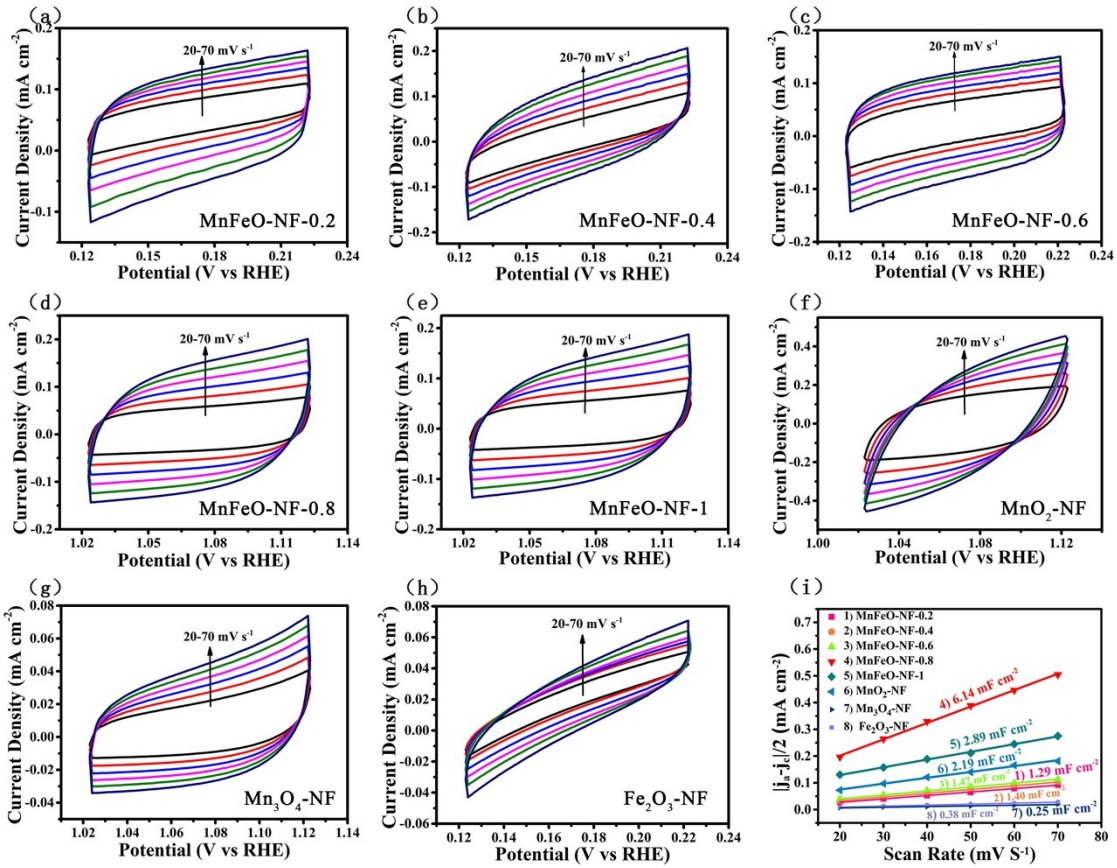

Fig. S11. CV curves at different scan rates for catalysts: (a) MnFeO-NF-0.2, (b) MnFeO-NF-0.4, (c) MnFeO-NF-0.6, (d) MnFeO-NF-0.8, (e) MnFeO-NF-1, (f) MnO_2-NF, (g) Mn_3O_4-NF, and (h) Fe_2O_3-NF. (i) Plots of capacitive currents with different scan rates for various catalysts to determine C_{dl}.

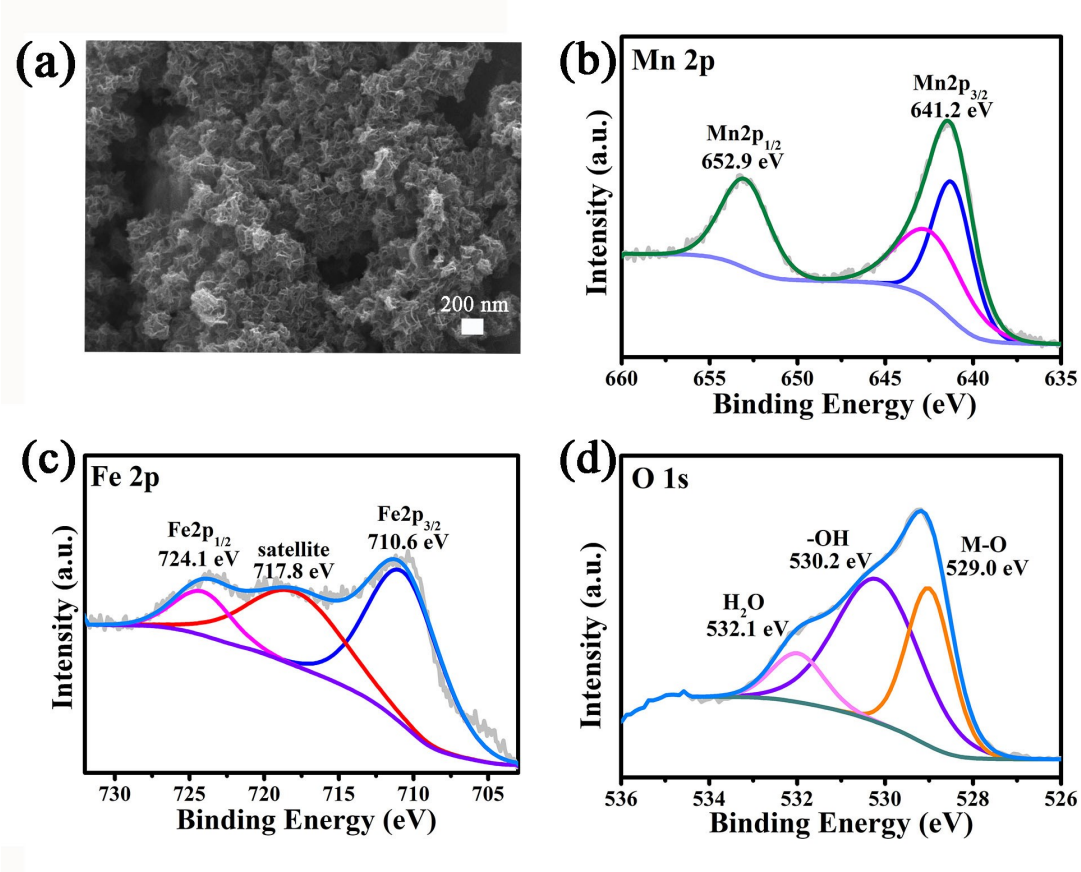

Fig. S12. (a) SEM image of MnFeO-NF-0.8 after stability test. (c-d) High resolution XPS spectra of Mn 2p, Fe 2p, and O 1s after stability test for MnFeO-NF-0.8.

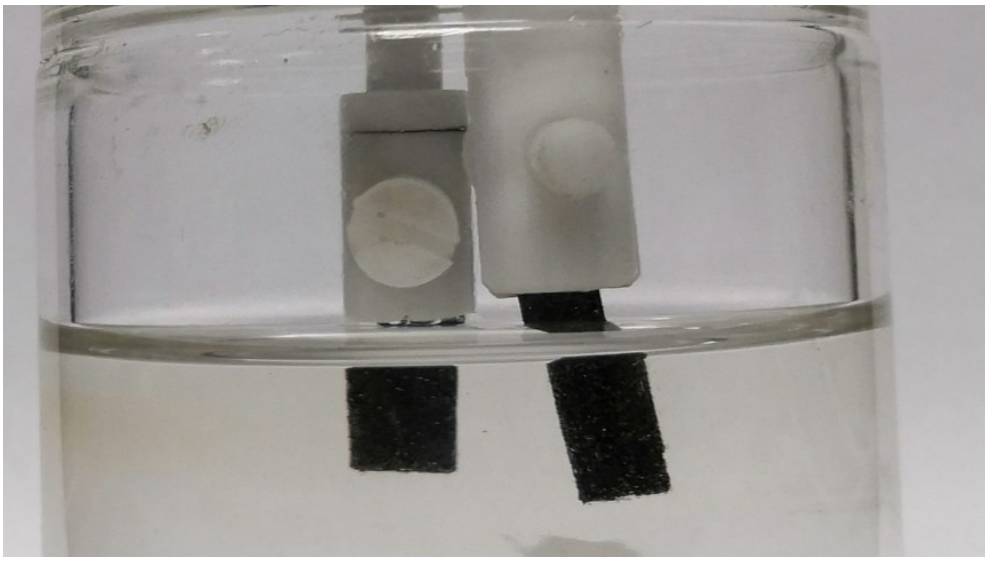

Fig. S13. Electrolyzation installation diagram of the MnFeO-NF-0.8 || MnFeO-NF-0.4.

Table S1. Comparison of the overpotentials for OER of different catalysts in this work.

Catalyst	η_{10} (mV)	η_{100} (mV)	η_{500} (mV)
MnFeO-NF-0.2	227	274	295
MnFeO-NF-0.4	157	225	257
MnFeO-NF-0.6	220	285	312
MnFeO-NF-0.8	243	319	356
MnFeO-NF-1	258	340	405
MnO_2-NF	342	433	464
Mn_3O_4-NF	339	438	481
Fe_2O_3-NF	318	432	--
NF	363	482	538

Table S2. Comparison of the overpotentials for HER of different catalysts in this work.

Catalyst	η_{10} (mV)	η_{100} (mV)	η_{500} (mV)
MnFeO-NF-0.2	186	295	347
MnFeO-NF-0.4	162	286	348
MnFeO-NF-0.6	153	235	314
MnFeO-NF-0.8	63	139	192
MnFeO-NF-1	143	231	280
MnO_2-NF	151	239	300
Mn_3O_4-NF	186	308	415
Fe_2O_3-NF	181	294	392
NF	171	270	326

Table S3. Comparison of activity for HER, OER, and overall water splitting of Mn_3O_4/Fe_2O_3/NF with other electrocatalysts in 1.0 M KOH.

Electrocatalyst	η for OER at target j (mV@mA cm^{-2})	η for HER at target j (mV@mA cm^{-2})	Voltage for OWS at target j (mV@mA cm^{-2})	Ref.
δ-MnO_2/NF	320@10	196@10	--	1
$(Fe_{1-x},Mn_x)OOH$	246@10	--	--	2
$Ni_{11}(HPO_3)_8(OH)_6/Mn_3O_4$	--	84@100	--	3
NiCoFe phosphate NSs-C/NF	240@10	231@10	1.52@10	4
NiFe/$NiCo_2O_4$/Ni Foam	340@1200	105@10	1.67@10	5
Hierarchical $NiCo_2O_4$	290@10	110@10	1.65@10-	6
Co@Co_3O_4	391@10	221@10	--	7
NiCo-nitrides/$NiCo_2O_4$/GF	183@10	71@10	1.68@20	8
$NiCo_2S_4$ NW/NF	260@10	210@10	1.63@10	9
$NiCo_2S_4/Ni_3S_2$/NF	--	119@10	--	10
Mn_3O_4/Fe_2O_3/NF	213@50	63@10	1.59@10	This work

References

1 Y. Zhao, C. Chang, F. Teng, Y. Zhao, G. Chen, R. Shi, G. I. N. Waterhouse, W. Huang and T. Zhang, *Adv. Energy Mater.*, 2017, **7**, 1700005.

2 M. P. Suryawanshi, U. V. Ghorpade, S. W. Shin, U. P. Suryawanshi, H. J. Shim, S. H. Kang and J. H. Kim, *Small*, 2018, **14**, 1801226.

3 Y. Tan, Q. Che and Q. Li, *J. Colloid Interface Sci.*, 2020, **560**, 714-721.

4 M. A. Z. G. Sial, H. Lin and X. Wang, *Nanoscale*, 2018, **10**, 12975-12980.

5 C. Xiao, Y. Li, X. Lu and C. Zhao, *Adv. Funct. Mater.*, 2016, **26**, 3515-3523.

6 X. Gao, H. Zhang, Q. Li, X. Yu, Z. Hong, X. Zhang, C. Liang and Z. Lin, *Angew. Chem. Int. Ed.*, 2016, **55**, 6290-6294.

7 C. Bai, S. Wei, D. Deng, X. Lin, M. Zheng and Q. Dong, *J. Mater. Chem. A*, 2017, **5**, 9533-9536.

8 Z. Liu, H. Tan, D. Liu, X. Liu, J. Xin, J. Xie, M. Zhao, L. Song, L. Dai and H. Liu, *Adv. Sci.*, 2019, **6**, 1801829.

9 A. Sivanantham, P. Ganesan and S. Shanmugam, *Adv. Funct. Mater.*, 2016, **26**, 4661-4672.

10 H. Liu, X. Ma, Y. Rao, Y. Liu, J. Liu, L. Wang and M. Wu, *ACS Appl. Mater. Interfaces*, 2018, **10**, 10890-10897.